Application of the DL-EPR – method for detecting sensitization to intergranular corrosion in thermomechanically rolled corrosion-resistant alloys 316L, 825L and 926L

M. Prohaska[1], T. Wernig[1], J. Perek[1], G. Mori[1], G. Tischler[2], R. Grill[2]

[1] *Christian Doppler Laboratory of Localized Corrosion, University of Leoben, Franz-Josef-Str. 18, 8700 Leoben, Austria,* manuel.prohaska@unileoben.ac.at

[2] *voestalpine Grobblech GmbH, Voest-Alpine-Straße 3, 4031 Linz, Austria*

The influence of a new thermo-mechanically rolling process (particularly end rolling temperature and cooling rate) on corrosion properties of three alloys (PREN values from 26 to 47) was studied by means of the DL-EPR – method and a conventional corrosion test ("Streicher-test" according to ASTM G28A). Prior to the measurement series, extensive optimization of the EPR – method was conducted for each material. Additionally, further characterization of corrosion properties was done by determination of "Critical Pitting Temperature" (according to ASTM G48C) and electrochemical measurements (current density – potential curves). Scanning electron microscopy (SEM) was used to characterize microstructure and type of attack after corrosion testing. A strong correlation between annual corrosion rates (examined by means of Streicher-test) and EPR-test results was obtained. With increasing PREN value the influence of rolling parameters on sensitivity to intergranular corrosion is elevated. This fact is related to a higher tendency of highly alloyed materials (especially of stainless steel 926L) to form various precipitates (carbides and/or intermetallic phases) in a temperature range between 700 and 1000 °C.

Key words: A. alloy 316L, B. alloy 825L, C. alloy 926L, D. EPR, E. intergranular corrosion

1. Introduction

The electrochemical potentiokinetic reactivation test (EPR) is a quasi non-destructive test to describe the corrosion resistance of stainless steels and nickel-based alloys. The EPR-method was developed by Cihal et al. [1] in 1969. Further improvements were achieved in the following decades [2]. This test is employed primarily to determine the degree of sensitization (DOS), i.e. the materials susceptibility to intergranular attack, but can also provide information on the general corrosion resistance and how this is affected by microstructural changes [3]. Compared to conventional corrosion tests, the EPR-test exhibits a couple of advantages: It is much quicker, more sensitive and more accurate, particularly for less sensitized specimens. Two different types of the EPR-test are common, the double loop and the single loop test. In the single loop EPR-test the polarization curve is a reverse curve, with a potential scan from the passive range to open circuit potential (OCP). In contrast, the double loop EPR-test shows a cyclic polarization curve consisting of a forward scan followed by a reverse scan starting at active OCP. For stainless steels 304 and 304 L the EPR-test parameters are prescribed in ASTM G108 [4].

The materials 316L, 825L and 926L are austenitic FeCrNiMo-alloys which are used in several industrial sectors (e.g. oil and gas industry, desalination and desulphurization plants as well as refineries) which require materials with outstanding corrosion properties combined with high strength at preferably low costs. One approach to achieve that aims is the manufacturing of composite materials consisting of a cheap base material, e.g. carbon or low-alloyed steel (to provide excellent mechanical properties) and of an expensive plating material with outstanding corrosion resistance. All materials investigated in this work were produced by means of a roll cladding process invented by Voestalpine Grobblech GmbH in Linz, Austria [5].

2. Experimental method

2.1. Chemical compositions, rolling parameters and heat treatments of materials 316L, 825L and 926L

The investigations included in this paper were conducted on sensitized, non-sensitized and thermo-mechanically rolled conditions. The chemical compositions as well as the chosen heat treatments (electric furnaces under ambient air were used) and rolling parameters are shown in tab. 1 and tab. 2. All materials were subjected to identical heat treatments and therefore, the designation "material" was used in tab. 2

instead of “316L”, “825L” and “926L”. Solution annealed and isothermally annealed specimens were investigated to have a good and a bad benchmark of corrosion properties.

Tab. 1: Chemical composition of Alloy 316L, 825L and 926L (in weight-%)

material	material number	C	Si	Mn	Cr	Ni	Mo	Cu	V	Ti	Co	Fe	N
316L	1.4432	0.01	0.32	1.56	16.74	10.52	2.58	0.31	0.05	-	0.24	67.50	0.03
825L	2.4858	0.01	0.22	0.76	22.10	39.80	3.04	1.81	0.09	0.74	0.15	45.50	-
926L	1.4529	0.01	0.36	0.95	20.30	24.90	6.44	0.94	0.03	-	0.12	30.80	0.21

Tab. 2: Heat treatments conducted on alloys 316L, 825L and 926L

sample description	thermo-mechanically rolled		isothermally annealed	
	end rolling temperature [°C]	cooling media	temperature [°C]	time [h]
material_SA	-	-	-	-
material_760_20	-	-	760	20
material_850_W	850	water	-	-
material_850_A	850	air	-	-
material_950_W	950	water	-	-
material_950_A	950	air	-	-

2.2. Testing methods

All sample conditions have been investigated by means of Streicher-test (according. to ASTM G28A), DL-EPR-test, current density - potential curves and, in case of alloys 825L and 926L, additional characterization of corrosion properties was done by determination of “Critical Pitting Temperature” (CPT – according to ASTM G48C).

2.3. Test solution

Streicher-test solution (used for all sample conditions) was composed of 236 ml sulfuric acid (H_2SO_4), 25 g iron (III) sulfate hydrate ($Fe_2(SO_4)_3.xH_2O$) and 400 ml distilled water (according ASTM G28A).
One litre of the used EPR-test solution was composed of different amounts of sulfuric acid (H_2SO_4), hydrochloric acid (HCl) and of potassiumthiocyanate (KSCN) as an activator (0 or 0.001 mol/l) mixed with reagent-grade distilled water. For each material, manifold EPR-solutions have been tested prior the measurement series to ensure high resolution of the DL-EPR-test regarding intergranular corrosion on the one hand and avoidance of uniform corrosion during the test on the other hand. Tab. 3 shows the optimized test solutions for each material investigated.

Tab. 3: Composition of optimized EPR-test solutions

material	conc. H_2SO_4 (98%) [ml/l]	conc. HCl (37%) [ml/l]	conc. KSCN [mol/l]
316L	28	6	0.001
825L	73	45	-
926L	73	60	0.001

For determination of CPT, the test solution was composed of 68.72 g reagent-grade ferric chloride ($FeCl_3 \cdot H_2O$) which was dissolved in 600 ml reagent-grade distilled water. Additionally, 16 ml of reagent-grade HCl (37%) was added. As a result, a solution containing about 6 % FeCl and 1 % HCl was produced.
Current density-potential curves were measured in an artificial brine containing 27 g/l NaCl at 80 °C and 1 bar CO_2 to simulate conditions during oil and gas production.

2.4. Test procedure

Prior the measurement series, all specimens were cut to 45x20 mm (Streicher-test), 10x10 mm (EPR-test) and 25x20 mm (CPT), respectively. The thickness of all thermo-mechanically rolled specimens was approximately 2 mm, whereas the thickness of all isothermally annealed specimens was 4 mm.
To evaluate the type of corrosive attack after testing, all Streicher- and EPR-test samples were surface-finished using final 1200-grit abrasive SiC-paper followed by polishing with 3 microns diamond suspension. All CPT-test specimens were surface-finished using final 120-grit abrasive SiC-paper.

After pouring the EPR-solution into the electrochemical cell, a delay of approx. 40 min was maintained to assure homogenous temperature of the test solution. Argon was used to stir the solution during the experiment to ensure an oxygen-free electrolyte.
It had to be considered that the EPR-test was started after a maximum delay of 3 minutes after polishing and cleaning with acetone to avoid the formation of an overly thick protective oxide layer on the samples' surface before immersing into the test solution. This oxide layer was found to have an essential impact on both activation current density (Ia) and reactivation current density (Ir).
Additionally, all EPR-test parameters were selected in a way to allow formation of an adequate thick passive layer during the test. Thus, dissolution of chromium/molybdenum depleted zones adjacent grain boundaries was enabled, but only eligible dissolution of non-sensitized specimen areas (interior the grains) occurred. The chosen test parameters are presented in tab. 4 and their selection was based on recent investigations [6].

Tab. 4: Optimized EPR-test parameters

material	scan rate [mV/s]	vertex potential [mV_{SCE}]	solution temperature [°C]
316L	1.66	+0	30
825L	1.66	+200	30
926L	1.66	+150	35

Before polarizing the samples during the EPR-test, the open circuit potential (OCP) was measured for 2 min. Besides, there was no delay at the vertex potential.
The current density ratio (Ir/Ia) as well as the charge density ratio (Qr/Qa) - in case of Alloy 316L and Alloy 825L - was calculated and evaluated.

The Streicher-test procedure was carried out strictly according to ASTM G28A.
CPT-test procedure was carried out strictly according to ASTM G48C.

Optical microscopy (type Zeiss "Axio Imager") was used to evaluate the most suitable EPR-test parameters by examining the extent of uniform corrosive attack in comparison to the extent of intergranular corrosive attack previous the measurement series. In addition, optical microscopy was used to measure the depth of pits after testing for determination of CPT.
All Streicher- and EPR-samples were additionally analysed by scanning electron microscopy. The microscope used for the current investigations was a Zeiss Instruments, type "Evo 50".

3. Results

3.1. Corrosion tests

Fig. 1 shows the results of Streicher-tests as well (fig. 1a) as EPR-tests (fig. 1b) of Alloy 316L. It is obvious, that both test methods show comparable results. The annual corrosion rate evaluated by means of Streicher-tests (except those of specimen 760_20) was approximately 1 mm. All thermo-mechanically rolled specimens exhibit (compared to the solution annealed condition) equal (Streicher) or even better (EPR) test values. In comparison to the other thermo-mechanically rolled conditions, a marginally lower current density ratio was examined for condition 850_W. As expected, the isothermally annealed condition is clearly worse compared to the other test conditions.

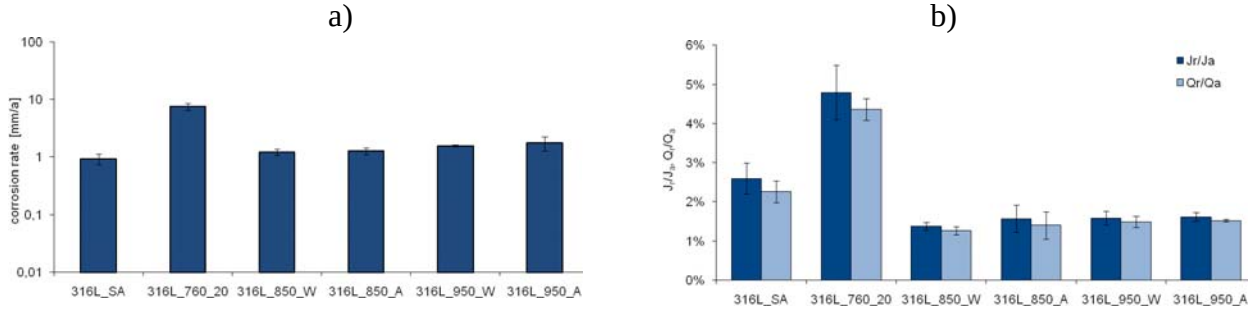

Fig. 1: Corrosion rate of Streicher-test (a) and Jr/Ja (Qa/Qr) values of EPR-test (b) of Alloy 316L

Fig. 2 shows the results of Streicher-tests as well (fig. 2a) as EPR-tests (fig. 2b) of Alloy 825L. The annual corrosion rate of all Streicher-specimens is about 0.2 mm. The current density ratios of all thermo-mechanically rolled conditions are equal compared to the solution annealed condition. The current density ratio of the isothermally annealed condition (760_20) is considerably higher compared to those of solution annealed and thermo-mechanically rolled conditions.

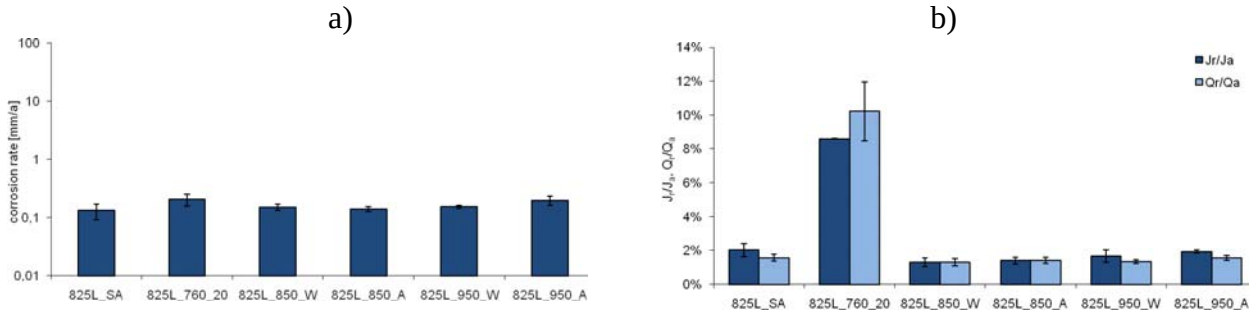

Fig. 2: Corrosion rate of Streicher-test (a) and Jr/Ja (Qa/Qr) values of EPR-test (b) of Alloy 825L

The investigated material conditions of Alloy 926L exhibit considerable differences in both annual corrosion rate (fig. 3a) and current density ratio (fig. 3b). The lowest corrosion rates exhibit both the solution annealed and one thermo-mechanically rolled condition (950_W) whereas the highest corrosion rate was evaluated for the isothermally annealed condition. EPR-results are in confirmation with Streicher-results, with one exception: The current density ratios of the isothermally annealed and the worst thermo-mechanically rolled condition (850_A) are in the same range.

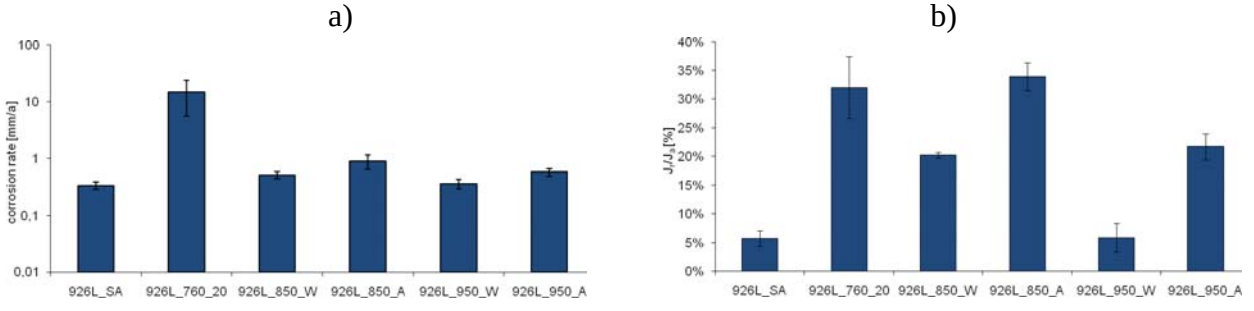

Fig. 3: Corrosion rate of Streicher-test (a) and Jr/Ja values of EPR-test (b) of Alloy 926L

Current density-potential curves of Alloy 316L are shown in fig. 4. All conditions exhibit a more noble repassivation potential compared to the corresponding open circuit potential (OCP). The OCP's of 760_20, 850_W, 850_A and 950_A are less noble compared to condition SA and 950_W. The pitting potentials of all conditions are between -50 (760_20) and +100 mV_{SCE} (950_W).

Fig. 5 describes the corrosion properties of Alloy 825L evaluated by means of current density-potential curves. It can be seen that all OCP values are between -150 and +70 mV_{SCE} and the corresponding repassivation potentials are slightly more noble. The pitting potentials of solution annealed and isothermally annealed condition are approx. 150 mV less noble compared to all thermo-mechanically rolled conditions.

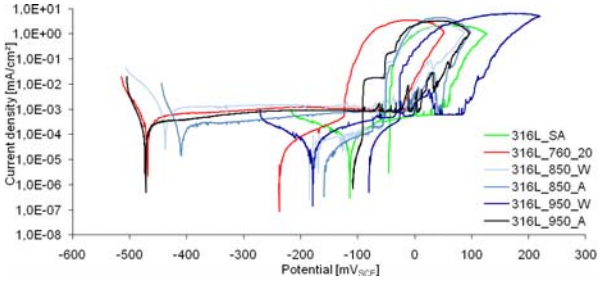

Fig. 4: I-U-curves of Alloy 316L (27 g/l NaCl, 80 °C, 600 mV/h, 1 bar CO_2)

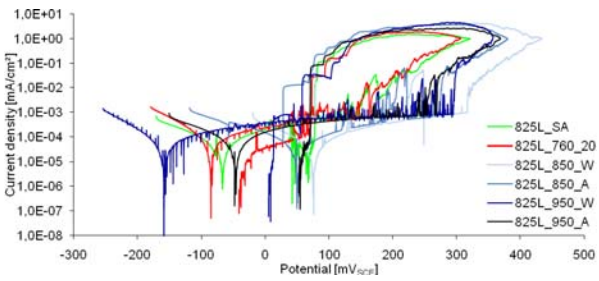

Fig. 5: I-U-curves of Alloy 825L (27 g/l NaCl, 80 °C, 600 mV/h, 1 bar CO_2)

Fig. 6 presents current density-potential curves of Alloy 926L. All curves exhibit a wide passive region (approx. 1100 to 1300 mV, with exception of 760_20 with a passive region of 500 mV) and OCP's from -450 to -100 mV_{SCE}. With respect to corrosion properties both the solution annealed specimens and the condition 950_W in particular show the best performance (small hysteresis, which means marginal localized corrosion and repassivation potentials of 700 and 900 mV_{SCE}, respectively). All the rest of the investigated conditions exhibit a higher extent of localized corrosion, which is attributed to large hysteresis during the measurements and considerably lower repassivation potentials (between -250 and +250 mV_{SCE}). The worst thermo-mechanically rolled condition is 850_A and the worst condition altogether is 760_20.

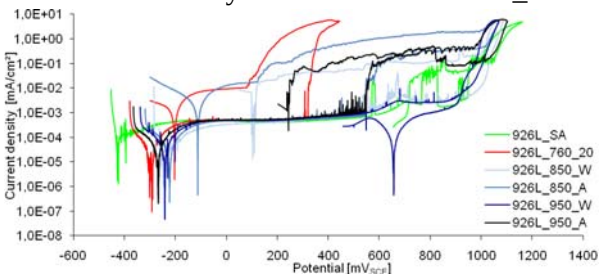

Fig. 6: I-U-curves of Alloy 926L (27 g/l NaCl, 80 °C, 600 mV/h, 1 bar CO_2)

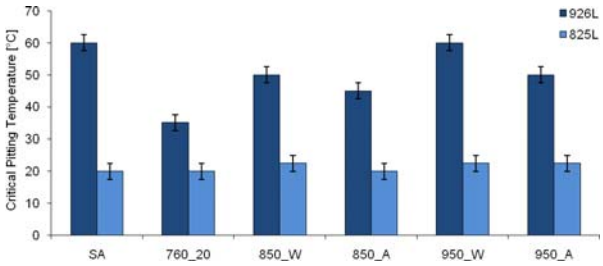

Fig. 7: CPT evaluation of Alloy 825L and 926L

In case of Alloy 825L and Alloy 926L additional characterization of corrosion properties was done by means of CPT evaluation. The results are illustrated in fig. 7. It is obvious that all conditions (even the isothermally annealed condition 760_20) exhibit CPT values around 20 °C and there is no noticeable dependency of CPT on material conditions.
Contrarily, the heat treatment parameters have a large impact on pitting resistence of Alloy 926L. The highest CPT values (60 °C) were determined for the solution annealed and the 950_W condition, whereas the lowest CPT value (35 °C) was examined for condition 760_20. The CPT values of the other thermo-mechanically rolled conditions are in the range of 45 to 50 °C.

3.2. Microstructural Characterization

Microstructural Characterization of selected specimens of Alloy 825L and Alloy 926L was done by means of scanning electron microscopy (SEM) after Streicher- and EPR-testing. Alloy 316L has not been investigated since no noticeable attack after Streicher- and EPR-testing was obtained.
Fig. 8 shows the morphology and the type of corrosive attack of Alloy 825L after Streicher-tests and EPR-tests. The conditions SA (fig. 8a) and 850_W (fig. 8c) show after Streicher-testing exclusively grain boundary attack, whereas after isothermal annealing (fig. 8e) additional localized attack interior the grains was observed.

After EPR-testing the samples SA (fig. 8b) and 850_W (fig. 8d) exhibit marginal grain boundary attack. Several small corrosion pits (size below 1 micron) were observed on specimen 850_W. In comparison to that noticeable larger corrosion pits were determined on condition 760_20 (size approx. 2-3 microns – fig. 8f).

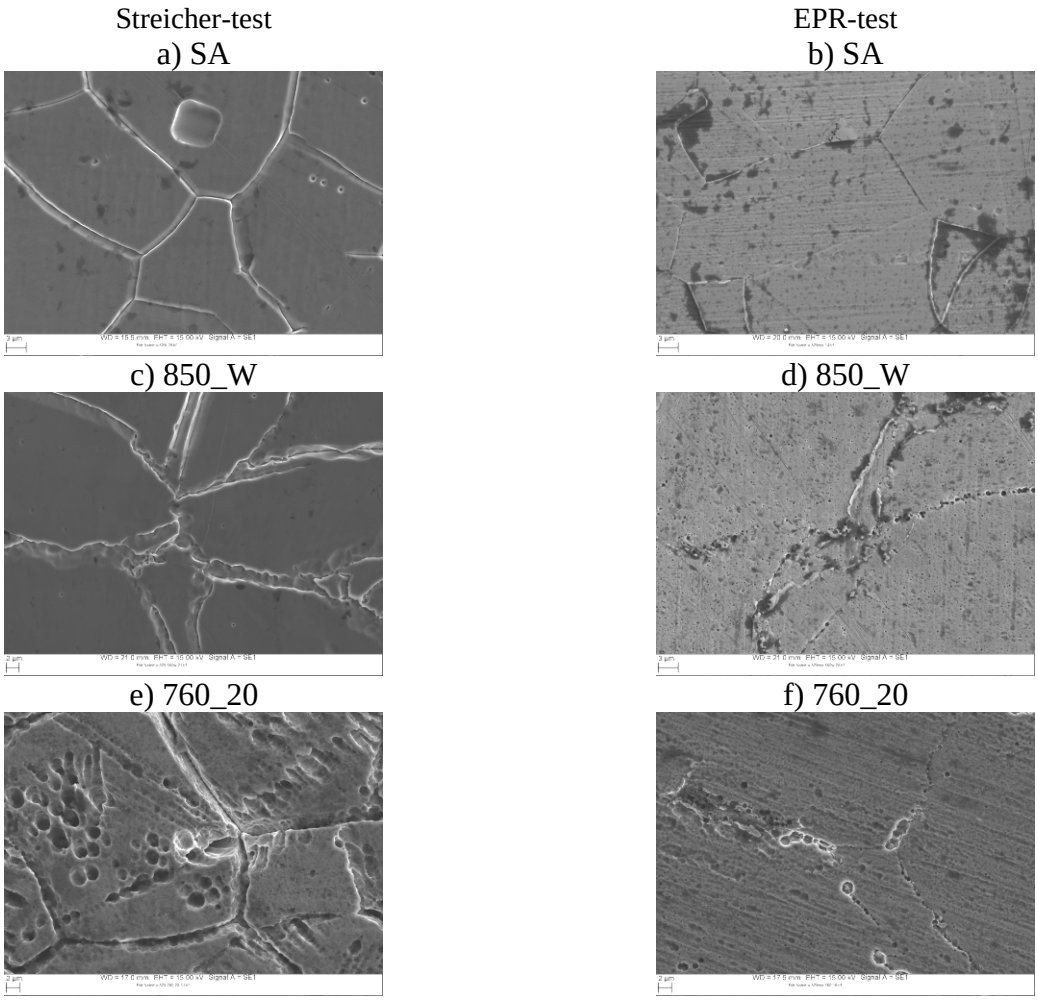

Fig. 8: SEM-images (SE) of 825L_SA, 825L_850_W and 825L_760_20 after Streicher-test and EPR-test

Fig. 9 shows the morphology and the type of corrosive attack of Alloy 926L after Streicher-tests and EPR-tests. The solution annealed sample shows deep and wide intergranular attack after Streicher-testing (fig. 9a). Contrarily, the best and the worst thermo-mechanically rolled samples (950_W and 850_A, respectively) exhibit a highly deformed surface where material dissolution occurred preferably along grain boundaries. The extent of attack was strongest after end rolling at 850 °C and air quench (fig. 9e).
After EPR-testing almost no intergranular attack was observed for conditions SA and 950_W, whereas a high extent of intergranular attack occurred in case of condition 850_A.

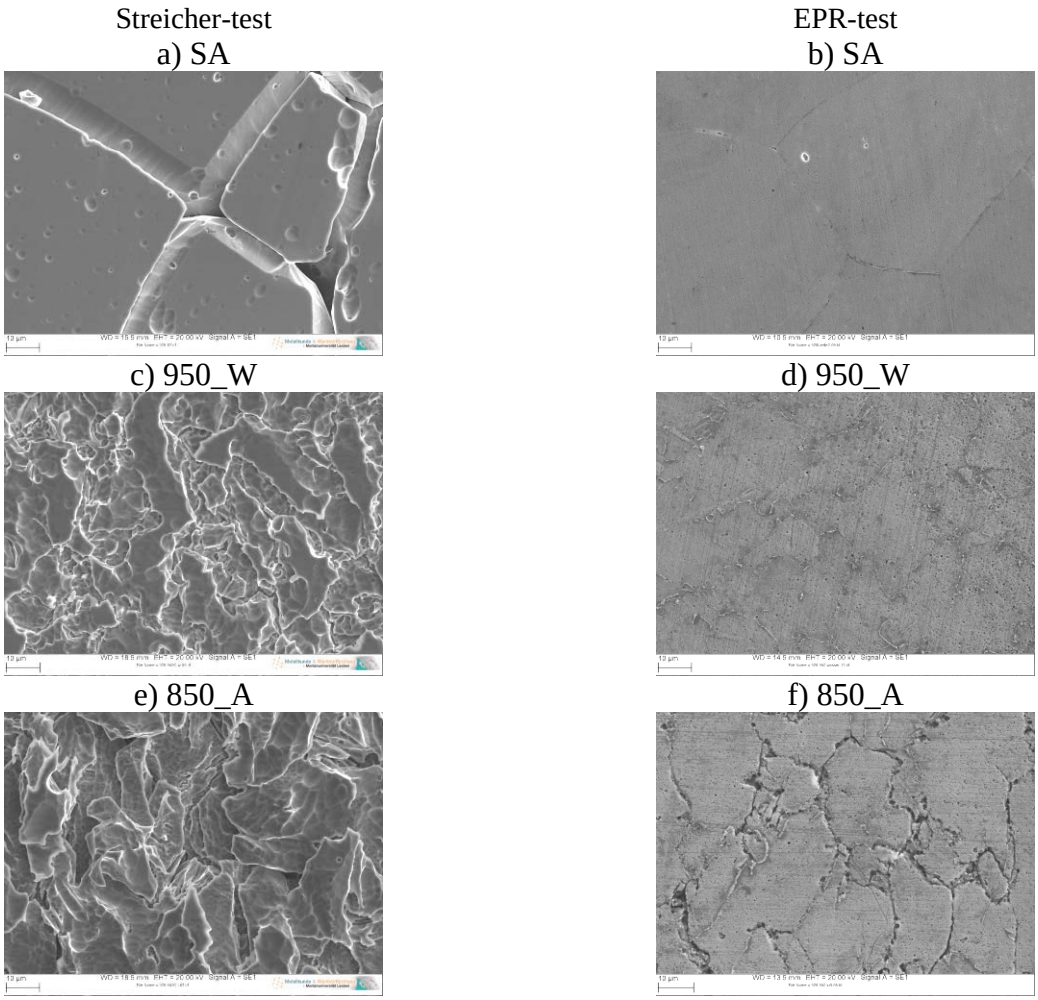

Fig. 9: SEM-images (SE) of 926L_SA, 926L_950_W and 926L_850_A after Streicher-tests and EPR-tests

4. Discussion

Both Streicher- and EPR-test evaluation showed that the influence of the production parameters on corrosion properties of thermo-mechanically rolled materials 316L and 825L is rather small compared to Alloy 926L.

For 316L and 825L the most promising production route is end rolling at 850 °C with subsequent water cooling especially when considering the resulting mechanical properties of carbon steel base materials of cladded sheets (fig. 1 and 2). However, no significant reduction in corrosion properties has to be expected when the cooling rate is smaller (air quench) and/or the end rolling temperature is higher (up to 950 °C). This assumption was supported by measuring current density-potential curves of both alloys (fig. 4 and 5). In both cases, the lowest corrosion resistance was observed after isothermal annealing at 760 °C for 20 h. This fact was referred to chromium and molybdenum carbide precipitation along grain boundaries after this type of heat treatment [7]. The precipitation of carbides leads to chromium and/or molybdenum depleted zones adjacent the grain boundaries and therefore, to an elevated sensitization to intergranular corrosion [8,9]. The presence of a considerable amount of carbides is confirmed by the morphology of the corrosive attack (determined by means of SEM), which is increasingly localized (fig. 8e) and spherical (fig. 8f).
When comparing the annual corrosion rates of Alloy 316L and Alloy 825L it is striking that the corrosion rates of Alloy 825L are significantly lower due to its high nickel content (extent of uniform corrosion is dramatically reduced).

In case of Alloy 926L a strong impact of the production route on resulting corrosion properties was observed. The most promising combination of end rolling temperature and cooling rate to avoid sensitization to intergranular corrosion is the condition 950_W. This condition shows after all corrosion investigations (Streicher-, EPR- and CPT-test plus current density-curves) equivalent results when compared to the solution annealed reference material. It was observed that a high cooling rate is essential to achieve remarkable

corrosion properties. Additionally, a high end rolling temperature yields to a smaller extent of intergranular corrosion.
The outcome of this work with respect to an applicable process window for Alloy 926L is in confirmation with the precipitation area of an intermetallic phase, the so-called chi-phase. This phase is rich in chromium and molybdenum and leads in consequence to chromium and/or molybdenum depletion around this precipitates. Above 900 °C and at times shorter than approx. 1 h less chi-phase precipitation takes place [10]. Thus, the outstanding corrosion properties of condition 950_W can be explained and confirmed.

5. Conclusions

The higher the PREN-value of the investigated alloys, the better is the resistance against general and localized corrosion. Though users should have in mind that with increasing PREN-value (which means an elevated content of chromium and molybdenum in particular) the tendency to form various precipitates (carbides and/or intermetallic phases) is elevated. This results in a high sensibility to process parameters (end rolling temperature and cooling rate) for highly alloyed corrosion resistant materials like Alloy 926L. If the chosen production route passes the precipitation areas of chromium- and molybdenum-rich precipitates, the corrosion properties are dramatically reduced.

EPR-test is a powerful tool to characterize degree of sensitization of corrosion resistant alloys within a short period of time. However, to achieve correct and reliable results, all test parameters have to be optimized for each material separately.

6. References

[1] V. Cihal, T. Shoji, V. Kain, Y. Watanabe, R. Stefec, Electrochemical Polarization Reactivation Technique: EPR – A Comprehensive Review, Fracture and Reliability Research Institute, Graduate School of Engineering, Tohoku University, 2004.
[2] V. Cihal, Intergranular Corrosion of Steels and Alloys, Elsevier Science Publishers, BV, 1984. Pp. 368.
[3] U. Mudali, R. Dayal, J. Gnanamoorthy, P. Rodriguez, Relationship between Pitting and Intergranular Corrosion of Nitrogen-bearing Austenitic Stainless Steels, ISIJ International 36 (1996) 799–806.
[4] Annual Book of ASTM Standards; Section 3: Metals Test Methods and Analytical Procedures, vol. 03.02, Wear and Erosion, Metal Corrosion, 2000.
[5] R. Schimböck, G. Heigl, R. Grill, T. Reichel, J. Beissel, U. Wende, Clad Pipes for the Oil and Gas Industry – Manufacturing and Applications, stainless steel world 2004, paper no. P0435 (2004), 1-19
[6] M. Prohaska, T. Wernig, G. Mori, G. Tischler, R. Grill, Possibilities and limitations of replacing a conventional corrosion test with an electrochemical potentiokinetic reactivation method using the example of alloy 625, EuroCorr (Nizza, France, 06-10 September 2009), paper no. 7901, 1–13.
[7] H. Sahlaoui, K. Makhlouf, H. Sidhoma, J. Philibert, Effects of ageing conditions on the precipitates evolution, chromium depletion and intergranular corrosion susceptibility of AISI 316L: experimental and modeling results, Materials Science and Engineering A 372 (2004) 98–108.
[8] Y.M. Pan, D.S. Dunn, G.A. Cragnolino, N. Sridhar, Grain-boundary chemistry and intergranular corrosion in alloy 825, Metallurgical and Materials Transactions A 31A (4) (2000) 1163–1173. 462
[9] H. Sahlaoui, H. Sidhom, J. Philibert, Prediction of chromium depleted-zone evolution during aging of Ni–Cr–Fe alloys, Acta Materialia 50 (2002) 1383– 1392.
[10] U. Heubner, M. Rockel, E. Wallis, Das Ausscheidungsverhalten von hochlegierten austenitischen Stählen mit 6% Molybdän und der Einfluss auf das Korrosionsverhalten, Werkstoffe und Korrosion 40 (1989)